Research Article

Yaqiong Li, Lifeng Zhang*, and Di Pan

Removal of SiC and Si₃N₄ inclusions in solar cell Si scraps through slag refining

https://doi.org/10.1515/htmp-2022-0016 received October 04, 2021; accepted December 14, 2021

Abstract: Silicon was recovered from solar cell Si scraps through 42.5 mol% SiO_2 –42.5 mol% CaO–15 mol% Al_2O_3 slag refining. The motion behaviors of Si_3N_4 and SiC were observed *in situ* and real-time using a high-temperature laser confocal microscope, and the recovery of Si through slag refining was carried out at 1,500°C for 30 min. Results indicated that both SiC and Si_3N_4 inclusions were concentrated in the slag, and this work provides a clear framework for recycling and reusing solar cell Si scraps.

Keywords: Si₃N₄, SiC, slag refining, solar cell Si scraps

1 Introduction

Photovoltaic (PV) technology is an important source of clean energy generation [1], and its market is dominated by Si-based solar cells. PV technology is rapidly developing under the dual pressure of environmental pollution and energy crisis, resulting in high demand for Si feedstock and increased costs [2]. However, in the multicrystalline Si (mc-Si) directional growth and Si wafer sawing processes, approximately 30–50% of Si are lost as Si scraps and sawing waste [3,4], which are contaminated by metallic impurities and a large number of inclusions such as SiC and Si_3N_4 . Consequently, this wastes Si resources and further damages the environment. It is imperative to recover the Si from Si scraps and sawing waste for sustainability.

Many methods employed to separate SiC and Si_3N_4 inclusions from Si scraps and sawing waste include directional

* Corresponding author: Lifeng Zhang, School of Mechanical and Materials Engineering, North China University of Technology, Beijing, 100144, China, e-mail: zhanglifeng@ncut.edu.cn Yaqiong Li: School of Metallurgical and Ecological Engineering, University of Science and Technology Beijing, Beijing, 100083, China

Di Pan: School of Materials Science and Engineering, Dalian University of Technology, Dalian 116024, China

solidification, filtering method, electromagnetic separation technology, and slag refining. During the directional solidification [5,6], C shows a low segregation coefficient in Si [7], which is accumulated in the liquid Si. Once the C content exceeds its solubility limit, SiC is then precipitated in Si ingot. The engulfment of SiC can be improved if the Si growth rate is slow, but the processing time is prolonged, resulting in more C introduced into the Si melts from the atmosphere and heating elements in the furnace. Zhang and Ciftja [8] applied the filtering technique to remove SiC and Si₃N₄ inclusions from Si scraps using foam filters. The large inclusions were successfully eliminated, but some SiC inclusions smaller than 10 µm still remained in the refined Si. The electromagnetic separation technology [4,9,10] was first proposed by Kolin in the 1950s [11] and then developed as a promising method to separate nonmetallic or less conductive inclusions from melts. Damoah and Zhang [9] studied the effect of a high-frequency electromagnetic field on SiC removal from molten Si, and 99% of inclusions were separated from the Si matrix and accumulated on the top, bottom, and sidewalls of Si. Additionally, Jiang et al. [10] also found similar results concerning the electromagnetic separation of SiC, where the addition of Al promoted the removal of SiC. However, the movement of small particles was mainly governed by the liquid melt flow [12], so it is difficult to remove the small particles in the electromagnetic separation process. In addition to decreasing metallic impurities, the slag refining process is particularly useful in removing inclusions. Wang et al. [13] proposed separating inclusions from molten Si using molten slag. Our group measured the wettability between SiC and SiO₂–CaO–MgO, confirming that the contact angle of slag/SiC was smaller than that of Si/SiC [14]. Yang et al. [15] applied slag refining to recover 79.25% of Si from the diamond wire saw Si powder waste. Therefore, the slag refining is of great interest to separate inclusions and recover Si waste, but many aspects of this technique remain unexplained.

The present work investigated the SiC and Si_3N_4 inclusions within Si scraps and observed the inclusion motion behavior *in situ* and real-time using a high-temperature laser confocal microscope (HT-LSCM). New

experimental results on the effects of SiC and Si₃N₄ inclusions removal are discussed.

2 Experimental methods

2.1 Raw materials

Si scraps (size: $0.5-2\,\text{mm}$) were used as raw materials, which were cut from the top of mc-Si after the directional solidification process, followed by crushing treatment. It contained significant amounts of SiC lumps and Si_3N_4 rods.

The slag reagents used in the present study are all analytical grade, including Al_2O_3 , CaO, and SiO_2 . Each regent was weighed at the desired mass and mixed, followed by grinding for 30 min to form a homogeneous composition of 42.5 mol% SiO_2 –42.5 mol% CaO–15 mol% Al_2O_3 .

2.2 Experimental procedure

2.2.1 Observation of SiC and Si₃N₄ inclusions motion behavior

Observing SiC and $\mathrm{Si_3N_4}$ inclusions motion behavior *in situ* and real-time was carried out using a HT-LSCM (YONEKURA MFG. Co., LTD, VL2000DX-SVF18SP). Details of the equipment were reported in ref. [14]. 0.04 g Si particles and 0.04 g 42.5 mol% $\mathrm{SiO_2}$ –42.5 mol% CaO –15 mol% $\mathrm{Al_2O_3}$ slag powders were charged into a MgO crucible (I.D. = 6 mm), which in turn was placed on a Pt holder (Figure 1). The temperature was measured by a B-type thermocouple, which was in contact with the Pt holder.

The sample was heated to 1,500°C at 400°C·min⁻¹ under an Ar atmosphere and then maintained for 30 min. When the slag melted, the motion behavior of SiC and Si₃N₄ inclusions were observed using the confocal microscope, and the photos were recorded as a function of time.

2.2.2 SiC and Si₃N₄ separation from Si scraps via slag refining

SiC and Si_3N_4 inclusions were separated from Si scraps via slag refining using a resistance furnace under an Ar atmosphere. The Si scraps and 42.5 mol% SiO_2 –42.5 mol%

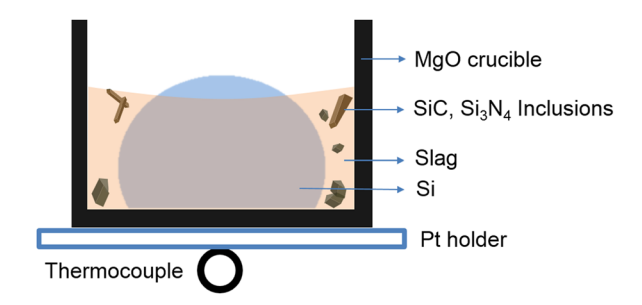


Figure 1: Schematic of the sample and sample holder in HT-LSCM.

CaO $-15 \, \mathrm{mol}\% \, \mathrm{Al_2O_3}$ slag with a mass ratio of 16:32 g were first charged in a high-purity graphite crucible (100 mm height and 30 mm inner diameter) and then placed inside the furnace. The temperature was measured using a B-type thermocouple and maintained at 1,500°C for 30 min. After the slag refining, the sample was withdrawn from the furnace and cooled in the air.

Moreover, the sample was cut vertically and then coated with Au film after the experiment, which was followed by SEM analysis.

3 Results and discussion

3.1 Si₃N₄ and SiC motion behavior

A small piece of Si particle was found on the top of the slag through the confocal microscopy, in which some black inclusions were distributed, as shown in Figure 2(a). Shifting the focus plane to the upper surface of the Si particle, the motion behavior of SiC and Si₃N₄ inclusions in Si and slag phases was observed during the heating process. The melting temperature of 42.5 mol% SiO₂-42.5 mol% CaO-15 mol% Al₂O₃ slag was approximately 1,335°C, calculated utilizing FactSage 7.1 software (equilibrium module; FToxid database), and it first melted as the temperature increased. When the temperature rose over 1,400°C, the Si started to melt (Figure 2(b)-(d)). As the amount of melted Si increased, the inclusions began to move freely (Figure 2(e)), and some inclusions collided to form a large inclusion cluster (Figure 2(f)-(g)). Once the inclusions in the melted Si approached and contacted the Si/slag interface, they were immediately absorbed and removed by the slag (Figure 2(h)). Similarly, inclusions were also trapped in molten slag (Figure 3). Previous results [14] indicated that the wettability of slag/SiC is better than that of Si/SiC, and the wettability of slag/Si₃N₄ can be viewed as perfect based on the present results.

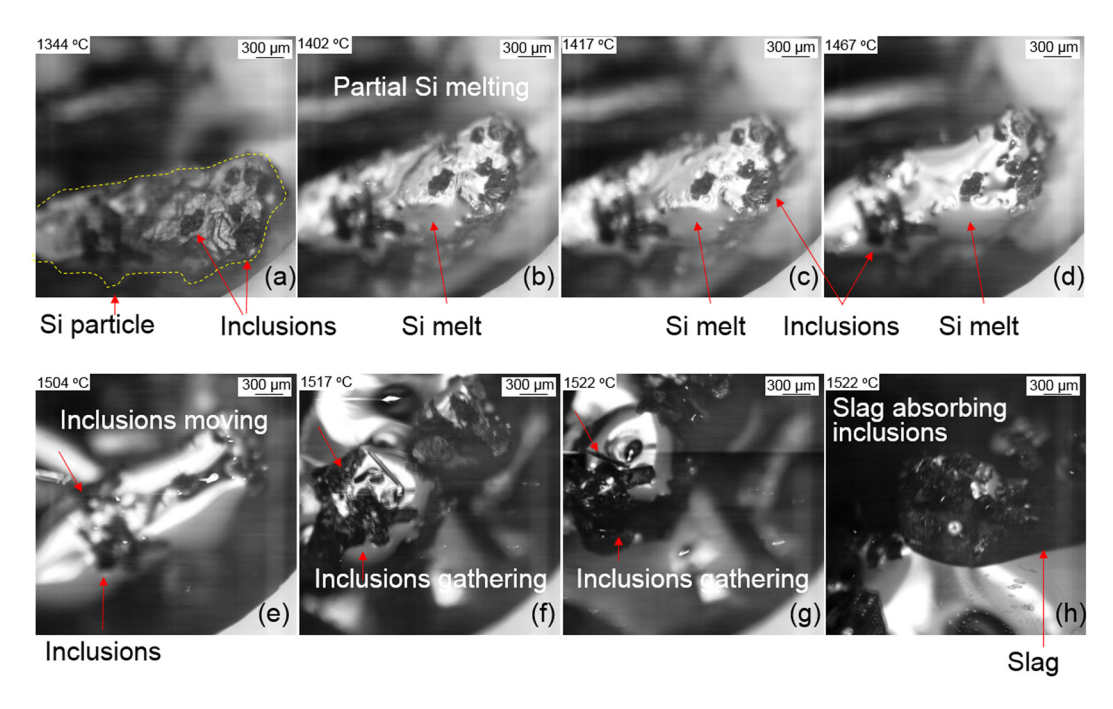


Figure 2: Motion behavior of Si_3N_4 and SiC inclusions in molten Si in the slag refining process. (a) Solid Si, (b)–(d) Si started to melt, (e)–(h) inclusions moved and trapped in the slag.

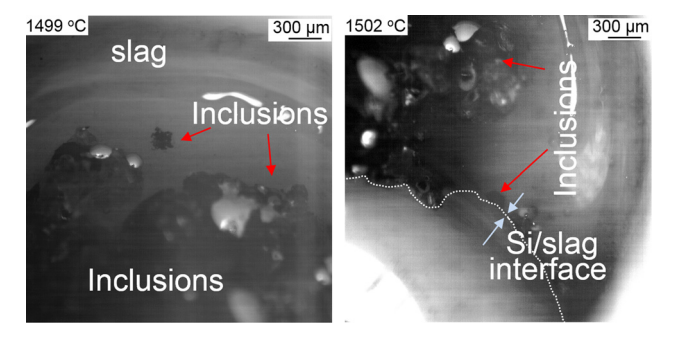


Figure 3: Motion behavior of Si_3N_4 and SiC inclusions in slag during the slag refining process.

3.2 Si₃N₄ and SiC removal through slag refining

Figure 4 shows the cross-sectional view of backscattered electrons images (BEI) of Si after slag refining. Several representative regions are chosen in Figure 4(a) and enlarged as shown in Figure 4(b)–(e). The Si block is placed above the slag which contains some dispersed Si droplets (Figure 4(a)). More SiC and Si_3N_4 inclusions indicated by black arrows are accumulated in regions A and B (Figure 4(b) and (c)), while only few are distributed in region C (Figure 4(d)). The findings demonstrated that

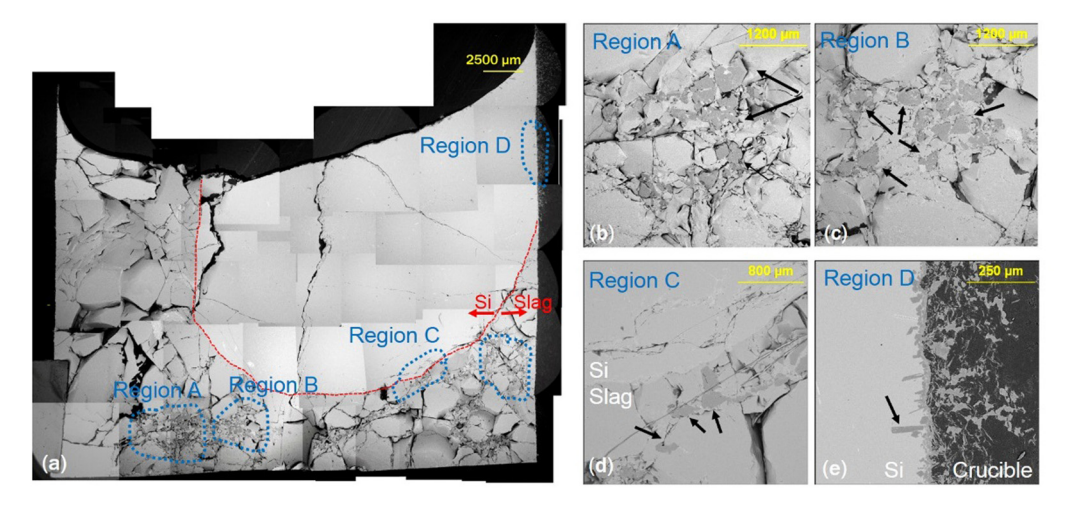


Figure 4: (a) Cross-sectional BEI image of the Si after slag refining and (b-e) enlarged BEI images of regions A-D in (a).

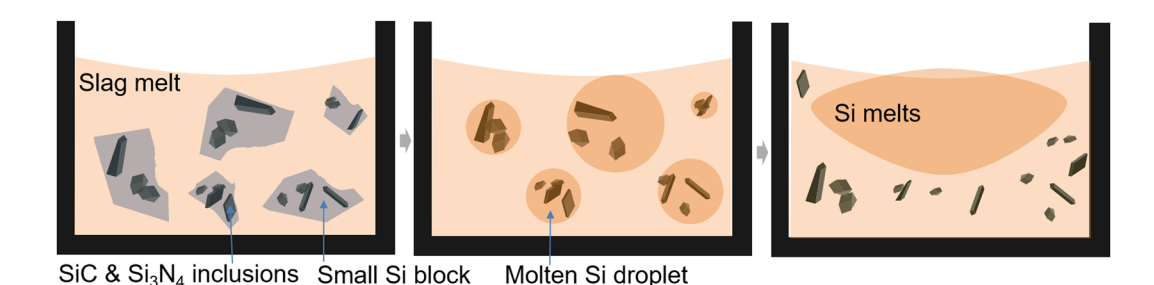


Figure 5: Schematic of Si recovery from solar cell Si scraps through slag refining.

the slag refining process was effective at removing SiC and Si_3N_4 inclusions. However, some SiC still existed in region D (Figure 4(e)), arranged as a layer in the inner side of the graphite crucible. No slag was found in region D, and the graphite crucible directly contacted the molten Si and introduced C into Si. The formation of the SiC layer is believed to be due to the chemical reaction between molten Si and graphite crucible, as expressed by equation (1).

$$Si(1) + C(1) = SiC(s).$$
 (1)

According to the experimental findings, the schematic of Si recovery from solar cell Si scraps through slag refining is shown in Figure 5. This process involves multiple steps: (1) the slag melts and surrounds the Si particles containing SiC and Si₃N₄ inclusions. (2) With the increase in the temperature, the Si melts, and the inclusions begin to move freely. Meanwhile, the Si droplets gather together. Once the particles encounter the slag/Si interface, they could be absorbed by the slag due to the excellent wetting behavior of SiC(Si₃N₄)/slag. (3) Several dispersed Si droplets melt together, and inclusions are captured in the molten slag. After slag refining treatment, the Si can be recovered from solar cell Si scraps.

4 Conclusion

The motion behavior of SiC and Si_3N_4 in Si and slag phases were observed *in situ* and in real-time using HT-LSCM, and they can be captured by the slag when they encountered the Si/slag interface. After slag refining, more SiC and Si_3N_4 inclusions were removed from molten Si. The application of slag refining to solar cell Si scraps can substantially reduce SiC and Si_3N_4 inclusions and finally recover Si.

Acknowledgements: The authors are grateful for support from the National Natural Science Foundation of China (No. 51604023), the Fundamental Research Funds for the

Central Universities (No. FRF-TP-20-035A2 and No. FRF-BD-20-04A), the High Steel Center (HSC) at Yanshan University, and Beijing International Center of Advanced and Intelligent Manufacturing of High Quality Steel Materials (ICSM), Beijing Key Laboratory of Green Recycling and Extraction of Metals and the High Quality Steel Consortium (HQSC) at University of Science and Technology Beijing (USTB), China.

Funding information: National Natural Science Foundation of China (No. 51604023), the Fundamental Research Funds for the Central Universities (No. FRF-TP-20-035A2 and No. FRFBD-20-04A).

Author contributions: Yaqiong Li: conceptualization, writing – original draft, funding acquisition, investigation, methodology; Lifeng Zhang: resources, supervision; Di Pan: methodology, software.

Conflict of interest: The authors declare that they have no known competing financial interests or personal relationships that could have appeared to influence the work reported in this article.

References

- [1] Chawla, R., P. Singhal, and A. K. Garg. Photovoltaic review of all generations: environmental impact and its market potential. *Transactions on Electrical and Electronic Materials*, Vol. 21, 2020, pp. 456–476.
- [2] Cañizo, C. D., G. D. Coso, and A. Luque. Ultrapurification of silicon for photovoltaic applications. Advances in Science and Technology, Vol. 74, 2010, pp. 99–106.
- [3] Satpathy, R. and V. Pamuru. Chapter 3 Silicon wafer manufacturing process. Solar PV power, Satpathy R. and V. Pamuru, eds, Academic Press, New York, 2021, p. 63.
- [4] Jiang, D., X. Li, S. Qin, J. Li, S. Shi, Y. Tan, et al. Separation of SiC from Si by addition of Al with electromagnetic induction melting. *Journal of Alloys and Compounds*, Vol. 835, No. 15, 2020, id. 155310.

- [5] Zheng, L., X. Ma, D. Hu, H. Zhang, T. Zhang, and Y. Wan. Mechanism and modeling of silicon carbide formation and engulfment in industrial silicon directional solidification growth. *Journal of Crystal Growth*, Vol. 318, No. 1, 2011, pp. 313–317.
- [6] Trempa, M., C. Reimann, J. Friedrich, and G. Müller. The influence of growth rate on the formation and avoidance of C and N related precipitates during directional solidification of multi crystalline silicon. *Journal of Crystal Growth*, Vol. 312, No. 9, 2010, pp. 1517–1524.
- [7] Davis Jr, J. R., A. Rohatgi, R. Hopkins, P. Blais, P. Rai-Choudhury, J. McCormick, et al. Impurities in silicon solar cells. *IEEE Transactions on Electron Devices*, Vol. 27, No. 4, 1980, pp. 677–687.
- [8] Zhang, L. and A. Ciftja. Recycling of solar cell silicon scraps through filtration, Part I: Experimental investigation. Solar Energy Materials & Solar Cells, Vol. 92, No. 11, 2008, pp. 1450–1461.
- [9] Damoah, L. N. W. and L. Zhang. High-frequency electromagnetic purification of silicon. Metallurgical and Materials Transactions B: Process Metallurgy and Materials Processing Science, Vol. 46, No. 6, 2015, pp. 2514–2528.
- [10] Jiang, D., S. Qin, P. Li, S. Shi, S. Wen, and Y. Tan. Electromagnetic separation of silicon carbide inclusions with

- aluminum penetration in silicon by imposition of supersonic frequency magnetic field. *Journal of Cleaner Production*, Vol. 145, No. 1, 2017, pp. 45–49.
- [11] Kolin, A. An electromagnetokinetic phenomenon involving migration of neutral particles. *Science*, Vol. 117, No. 3032, 1953, pp. 134–137.
- [12] Chen, W., Y. Ren, and L. Zhang. Large eddy simulation on the fluid flow, solidification and entrapment of inclusions in the steel along the full continuous casting slab strand. *JOM*, Vol. 70, No. 12, 2018, pp. 2968–2979.
- [13] Wang, D., Z. Wang, Z. Wang, G. Qian, X. Gong, and L. Xin. Silicon recovery from silicon sawing waste by removal of SiC impurity via CaO-SiO₂-Na₂O slag absorption. *Separation and Purification Technology*, Vol. 231, 2020, id. 115902.
- [14] Li, Y., Z. Li, L. Zhang, X. Wen, C. Ren, and Y. Yu. Silicon recovery from Si sawing waste through slag refining. Separation and Purification Technology, Vol. 274, 2021, id. 119065.
- [15] Yang, S., X. Wan, K. Wei, W. Ma, and Z. Wang. Investigation of Na₂CO₃-CaO-NaCl (or Na₃AlF₆) additives for the remanufacturing of silicon from diamond wire saw silicon powder waste. *Journal of Cleaner Production*, Vol. 286, 2021, id. 125525.